Nonaromatic Planar Si_{12} Ring System of Approximate D_{6h} Symmetry in $Ca_7Mg_{7.5\pm\delta}Si_{14}$

Reinhard Nesper,* Antonio Currao, and Steffen Wengert

Dedicated to Professor Hans-Georg von Schnering on the occasion of his 66th birthday

Abstract: $Ca_7Mg_{7.5\pm\delta}Si_{14}$ is the correct stoichiometry of the so called $Ca_7Mg_6Si_{14}$ of Gladishevskii et al.[1] $Ca_7Mg_{7.5\pm\delta}Si_{14}$ is an approximate or unusual Zintl phase with metallic conductivity that is expected to be highly anisotropic. The crystal structure (*P6/mmm* (no. 191), $a = 12.696(2)$, $c = 4.4025(5)$ Å, $Z = 1$) contains planar hexasilylhexasilacyclohexene anions (Si_{12}) of D_{6h} symmetry, with a formal charge of $-(21 \pm 2\delta)$, besides isolated Si_4^{4-} anions. Quantum mechanical calculations based on the Extended Hückel and LMTO-ASA methods establish metallic properties due to a $\pi^* - \pi^*$ interaction of the ecliptically stacked Si_{12} units. The planar ring system does not show aromaticity, but contains approximately 1.75 double bonds that are equally delocalized.

Keywords: conducting materials · crystal structure · electronic structure · electron localization function · silicon · Zintl phases

Introduction

We are studying ternary silicides $M_xM'_ySi$ because there is evidence that the ratio $x:y$ has a pronounced effect on the structure of the Zintl anions that occur at relatively high silicon contents. In general, such compounds are semiconductors and follow a generalized (8-*N*) rule, the so called Zintl–Klemm concept.[2–8] Therefore, if M and M′ do not belong to the same group of elements, for example, they transfer different numbers of valence electrons to the silicon cluster anions, a variation in the latter must occur according to the change in electronic structure. For the case that the metal components M and M′ belong to the same group and transfer the same number of valence electrons, more subtle effects determine the structure of the Zintl anions Si_{n-}^{m}; these arise from acid–base interactions, size factors, and electronegativity differences.

High-pressure experiments by Evers et al.[9–12] have shown that the structures of Zintl anions can be changed by application of fairly moderate external pressure. From a number of investigations we know that magnesium has quite a different effect on Zintl anions than the heavier alkaline earth metals calcium, strontium, and barium.[13, 14] Indications for this difference are already obvious from the comparison of the binary alkaline earth metal silicides. In the binary Mg/Si system only the saltlike Mg_2Si[15] is known, containing isolated Si^{4-} anions with a large formal charge transfer, while the heavier homologues form a number of binary silicides with different Zintl anions.

There are seven binary phases bordering the ternary system Ca/Mg/Si. Mg_2Si and the Laves-phase $CaMg_2$[16] are the only binary phases in their systems, while five well-characterized binary Ca/Si compounds have been reported. In Ca_2Si[17] isolated Si^{4-} anions are found. Ca_5Si_3[18] again contains isolated Si^{4-} together with Si_2^{6-} dumbbells. CaSi[19–22] forms planar $^1_\infty[Si^{2-}]$ chains, and in $CaSi_2$[10, 23, 24] corrugated layers of $^2_\infty[Si^-]$ are present. A two dimensional silicon framework is found in $Ca_{14}Si_{19}$.[25] There is a report on a sixth binary compound Ca_3Si_4,[26] but no structural data have been given. Our own investigations support the existence of isotypic binary and ternary compounds with the composition Ca_3Si_4 and $Ca_{(3-x)}Mg_xSi_4$, respectively.[27] The results concerning these investigations will be reported elsewhere. Currently, references to two ternary compounds can be found in the literature. CaMgSi contains isolated Si^{4-} anions and was characterized by single-crystal X-ray diffraction.[28, 29] With some diligence a Russian conference proceeding can be found that reports the existence of a ternary compound $Ca_7Mg_6Si_{14}$.[1] The lattice constants and overall structure given in this abstract reveal that the compound has to be identical to the

[*] Prof. Dr. R. Nesper, Dr. S. Wengert
Laboratorium für Anorganische Chemie, Eidgenössische Technische Hochschule Zürich
Universitätstrasse 6, CH-8092 Zürich (Switzerland)
Fax: (+41) 1-632-1149
E-mail: nesper@inorg.chem.ethz.ch

Dr. A. Currao
Kynshu, Reasearch Suku-machi 807 Saga-Ken (Japan)
E-mail: toni@kniri.go.jp

  0947-6539/98/0411-2251 $ 17.50+.25/0

one we present and thus has the stoichiometry $Ca_7Mg_{7.5\pm\delta}Si_{14}$. Here, δ is a measure of insecurity of the composition from the X-ray refinement rather than a measure of phase width, as we will outline in the following. Crystal structure analysis, magnetic and conductivity measurements, as well as quantum mechanical investigations based on the Extended Hückel (EHMO) and LMTO-ASA methods have been carried out.

Experimental Section

Preparation: $Ca_7Mg_{7.5\pm\delta}Si_{14}$ was prepared by direct synthesis from stoichiometric amounts of the elements in niobium ampoules (length: 45 mm; diameter: 15 mm; wall thickness: 1 mm). The ampoule was heated in a closed quartz tube under argon atmosphere up to 1120 K for 4 hours. According to differential thermal investigations the compound decomposes peritectically to the saltlike CaMgSi and elemental silicon above 1253 K. Decomposition and back formation of $Ca_7Mg_{7.5\pm\delta}Si_{14}$ was proved to be reversible by DTA and X-ray powder methods. No indication for shifts of X-ray lines or line broadening was observed. Thus, we believe that there is no significant phase width. For further purification of the compound, the primary product was crushed in a mortar and the resulting powder was pressed into a pellet (diameter: 13 mm; thickness: 2 mm), welded in a niobium ampoule (length: 35 mm), and heated up first to 1200 K for 5 hours and then kept for another 90 hours at 1070 K. The resulting sample is a nearly pure phase $Ca_7Mg_{7.5\pm\delta}Si_{14}$ with minor $CaSi_2$ impurity. Small gray single crystals with metallic luster could be separated from the pellet. The compound is stable in air for month, but reacts with diluted mineral acids under formation of silanes and amorphous silicon.

Results and Discussion

Physical properties: In order to get more information on the physical properties of the compound, magnetic and conductivity measurements were performed on pellets of the powdered material. To reduce the effects of grain boundaries the pellets (diameter: 13 mm; thickness: 3 mm) were heated up to 1070 K for another 10 hours in niobium ampoules. The conductivity measurements were performed with a square arrangement of four rhodium electrodes, which were pressed against the plane surface of the pellet. Two electrodes were used to apply a constant current of 0.1 A, and the other two electrodes were used to measure the voltage changes. The sample was cooled down by a closed circuit helium cryostat. Figure 1 shows a plot of the resistance versus temperature.

Isotropic susceptibility measurements were performed in the temperature range from 2 K to 300 K with a SQUID magnetometer (MPMS 5S, Quantum Design) in a field of 1 T. For the measurements a piece of the pellet was placed in a polyethylene sample holder. The material was found to be diamagnetic with a molar magnetic susceptibility of $\approx -9.0 \times 10^{-4}\,cm^3\,mol^{-1}$ at 300 K. If one takes into account the diamagnetic increments of the Ca^{2+} and the Mg^{2+} ions according to ref. [30], one will end up with a diamagnetic increment of $-59.0 \times 10^{-6}\,cm^3\,mol^{-1}$ for anionic silicon in $Ca_7Mg_{7.5\pm\delta}Si_{14}$ that is comparable with $-42.5 \times 10^{-6}\,cm^3\,mol^{-1}$ found for anionic silicon in $Ca_{14}Si_{19}$;[25] however, this compound is a classical Zintl phase containing only Si–Si single bonds. The delocalized π-systems of the Si_{12} unit may give rise to an enhanced diamagnetism, but it is not known to what extent. This must be subject of further investigations. At present no reliable guess is possible for a temperature independent Pauli paramagnetism, which would be expected for a metallic conductor. So far the magnetic properties are not in agreement with the resistivity measurements and the theoretical investigations discussed later.

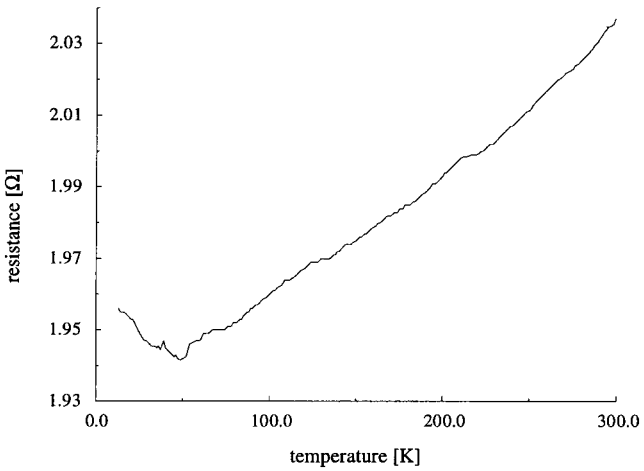

Figure 1. Temperature dependence of the resistance of $Ca_7Mg_{7.5\pm\delta}Si_{14}$.

Figure 2 shows a plot of the molar magnetic susceptibility versus the temperature. At about 50 K there is a change of slope in the χ versus T curve that is also matched by a change of slope in the temperature-dependent resistivity. This change may be an indication of a localization phenomenon at low temperatures.

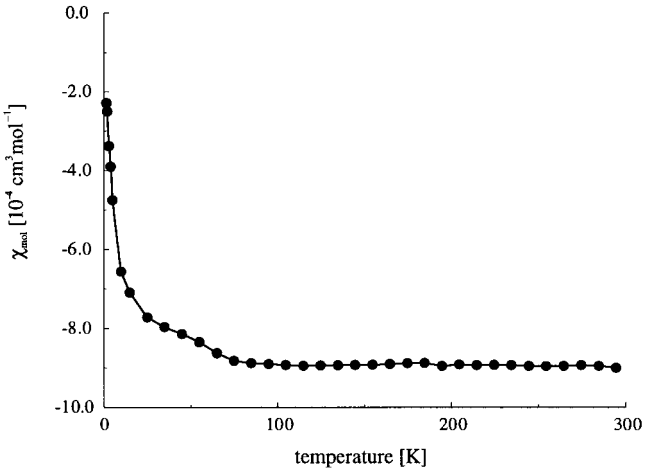

Figure 2. Temperature dependence of the molar magnetic susceptibility of $Ca_7Mg_{7.5\pm\delta}Si_{14}$.

Refinement and crystal structure: Data collection for $Ca_7Mg_{7.5\pm\delta}Si_{14}$ was performed on a four-circle diffractometer (STAD14, STOE) with graphite monochromator and $Mo_{K\alpha}$ radiation (0.71073 Å). Crystallographic data are summarized in Table 1.[31] Three standard reflections were checked every 180 minutes. Four unique sets were measured for the Laue group $6/m$. An empirical absorption correction (ψ-scan) with 10 reflections was carried out, and the data were corrected for

0947-6539/98/0411-2252 $ 17.50+.50/0 *Chem. Eur. J.* **1998**, *4*, No. 11

Table 1. Crystal data and structure refinement for $Ca_7Mg_{7.5\pm\delta}Si_{14}$.

formula	$Ca_7Mg_{7.6}Si_{14}$
M_r [g mol^{-1}]	856.6
T [K]	298(2)
crystal system	hexagonal
space group	*P6/mmm* (No. 191)
V [Å^3]	614.5(1)
a [Å]	12.696(2)
c [Å]	4.4025(5)
Z	1
ρ_{calcd} [g cm^{-3}]	2.315
absorption coefficient μ [mm^{-1}]	2.378
$F(000)$	423
crystal size [mm]	$0.15 \times 0.10 \times 0.05$
data collection	four-circle diffractometer STOE STADI 4, Learned Profile Method [51] with ω-θ scan
monochromator, wavelength	graphite, λ $Mo_{K\alpha} = 0.71073$ Å
2θ range	$2^\circ \le 2\theta \le 65^\circ$
index range	$-21 \le h \le 18$, $-21 \le k \le 18$, $0 \le l \le 7$
reflections collected	4874
independent reflections	692,[d] $R_{int} = 0.076$
absorption correction	Ψ scan
solution refinement method	SHELXS-86, SHELXL-96
data/restraints/parameters	692/0/29
reflections with $[F_o^2 > 2\sigma(F_o^2)]$	430
goodness of fit[e]	1.161
$R1$[a] $[F_o^2 > 2\sigma(F_o^2)]$	0.042
$wR2$[b] $[F_o^2 > 2\sigma(F_o^2)]$	0.069 ($a = 0.0068$; $b = 2.50$)
$R1$[a] (all data)	0.089
$wR2$[b] (all data)	0.089
largest difference peak/hole	2.31/−1.07 e Å^{-3}

[a] $R1 = \Sigma(F_o - F_c)/\Sigma F_o$. [b] $wR2 = \sqrt{\Sigma(w(F_o^2 - F_c^2)^2)/\Sigma w(F_o^2)^2}$, $w = 1/\sigma^2(F_o^2) + (aP)_2 + bP$, $P = (\mathrm{Max}(F_o^2,0) + 2F_c^2)/3$. [c] $\mathrm{GooF} = \sqrt{\Sigma(w(F_o^2 - F_c^2)^2)/(n-p)}$, n = no. of reflections, p = no. of parameters. [d] $R_{int} = (\Sigma F_o^2 - \bar{F}_o^2)/\Sigma F_o^2$. [e] $R_\sigma = \Sigma\sigma(F_o^2)/\Sigma F_o^2$

Lorentz and polarization effects. The structure was solved by Patterson methods with SHELXS86[32] and refined with SHELXL96.[33] Anisotropic displacement parameters were applied for all atoms in the final full-matrix least-squares calculations (Tables 2 and 3).

The crystal structure contains isolated silicon atoms and a planar Si_{12} group of D_{6h} symmetry (Figures 3 and 4). The calcium and silicon sites are fully occupied, whereas the magnesium positions are not. Both the occupation and displacement parameters of the Mg positions were refined freely and yielded a composition of $Ca_7Mg_{7.7(2)}Si_{14}$. Considering the forbidden short distances between Mg (split) positions, several constraints for combined occupancies can be formulated: common occupancies of Mg1−Mg3 and Mg3−Mg3

Table 2. Atomic coordinates, thermal displacement parameters (esd) [pm^2] and site occupation factors (esd) for $Ca_7Mg_{7.5\pm\delta}Si_{14}$. U_{eq} is defined as 1/3 of the trace of orthogonalized U_{ij}.

Atom	Site	x	y	z	U_{eq}/U_{iso}	Occupation
Ca1	1a	0	0	0	110(4)	1
Ca2	6l	0.1819(1)	2x	0	221(3)	1
Si1	6k	0.1820(1)	0	1/2	211(3)	1
Si2	6k	0.3648(1)	0	1/2	193(3)	1
Si3	2c	1/3	2/3	0	161(5)	1
Mg1	6m	0.4109(2)	2x	1/2	263(8)	0.591(6)
Mg21	3f	1/2	0	0	270(62)	0.150(15)
Mg22	6l	0.4683(3)	2x	0	180(10)	0.409(6)
Mg3	6m	0.2716(5)	2x	1/2	201(27)	0.178(7)

Table 3. Coefficients for anisotropic thermal displacement parameters (esd) for $Ca_7Mg_{7.5\pm\delta}Si_{14}$. U_{ij} are defined according to $\exp[-2\pi^2(U_{11}h^2a^{*2} + \cdots + 2U_{23}klb^*c^*)]$.

Atom	U_{11}	U_{22}	U_{33}	U_{12}	U_{13}	U_{23}
Ca1	119(5)	U_{11}	91(8)	0	0	1/2 U_{11}
Ca2	245(4)	274(6)	152(4)	0	0	1/2 U_{22}
Si1	104(5)	93(6)	432(9)	0	0	1/2 U_{22}
Si2	169(4)	367(8)	109(5)	0	0	1/2 U_{22}
Si3	136(6)	U_{11}	213(11)	0	0	1/2 U_{11}
Mg1	217(12)	249(17)	332(18)	0	0	1/2 U_{22}
Mg3	286(45)	164(46)	112(39)	0	0	1/2 U_{22}

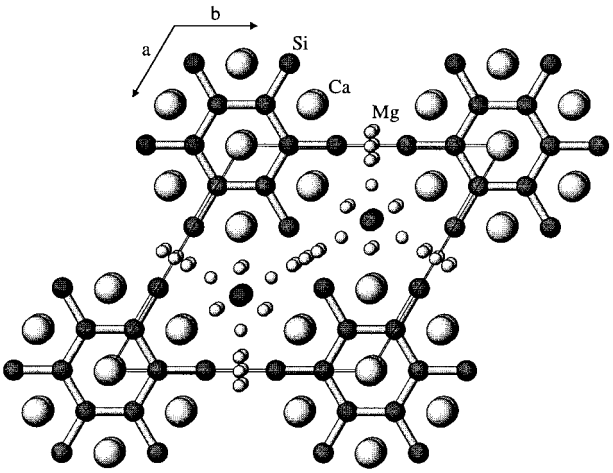

Figure 3. Perspective view on the crystal structure of $Ca_7Mg_{7.5\pm\delta}Si_{14}$ along [001].[48]

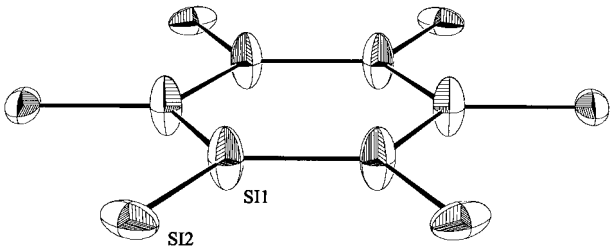

Figure 4. Geometry of the planar Si_{12} unit.[49]

are impossible (see Table 4). As the Mg3 positions form a small triangle, the resulting constraint is $2\,\mathrm{SOF(Mg3)} + \mathrm{SOF(Mg1)} \le 1$ (SOF = site occupation factor). This is fulfilled even in the free refinement. The second correlation of the split positions Mg21 and Mg22 allows for only one atom on the three neighboring positions giving rise to $\mathrm{SOF(Mg21)} + 2\mathrm{SOF(Mg22)} \le 1$, which is also a direct result of the unconstrained refinement. However, the Mg neighbor pairs Mg1 and Mg22 tend to be slightly over-occupied with respect to the necessary constraint $\mathrm{SOF(Mg1)} + \mathrm{SOF(Mg22)} \le 1$. The constraint refinement converges to reliability factors that are almost indistinguishable to those of the free refinement. The observed variations of the displacement parameters are within twice the standard deviations of the corresponding parameters, which are very reasonable for both cases. The constraint refinement yields a stoichiometry of $Ca_7Mg_{7.6(2)}Si_{14}$. The simplest ordered model that we could generate utilizes a fourfold unit cell ($a' = 2a$, $b' = 2b$, $c' = c$, see Figure 5) and yields a composition of $Ca_7Mg_{7.25}Si_{14}$, which is just within twice

Table 4. Atomic distances (esd) [pm] for $Ca_7Mg_{7.5\pm\delta}Si_{14}$; *n* denotes the frequency of the corresponding distance.

Atom pair	*d*	*n*	Atom pair	*d*	*n*	Atom pair	*d*	*n*
Ca1–Si1	319.1(1)	12	Si3–Mg3	258.6(6)	6	Mg22–Mg21	69.7(5)	
Ca1–Ca2	399.8(1)	6	Si3–Mg1	278.5(3)	6	Mg22–Mg22	139.3(10)	
			Si3–Mg22	296.8(5)	3	Mg22–Mg1	253.8(3)	2
Ca2–Mg3	295.6(7)	2	Si3–Ca2	333.0(2)	3	Mg22–Si2	287.7(2)	4
Ca2–Mg22	316.5(3)	2	Si3–Mg21	366.50(5)	3	Mg22–Si3	296.8(5)	
Ca2–Si1	318.9(1)	4				Mg22–Ca2	316.5(3)	2
Ca2–Si2	319.5(1)	4	Mg1–Mg3	156.1(4)	2	Mg22–Mg3	338.7(4)	4
Ca2–Si3	333.1(2)		Mg1–Mg22	253.8(3)	2	Mg22–Mg1	345.0(5)	2
Ca2–Mg21	351.0(1)	2	Mg1–Si2	260.5(3)	2	Mg22–Ca2	394.8(4)	2
Ca2–Mg1	362.8(1)	4	Mg1–Si3	278.5(3)	2			
Ca2–Mg22	394.8(4)	2	Mg1–Mg21	294.7(3)	2	Mg3–Mg1	156.1(4)	2
Ca2–Ca2	400.0(1)	3	Mg1–Mg1	295.4(6)	2	Mg3–Mg3	235.2(18)	2
			Mg1–Mg3	306.3(11)		Mg3–Si3	258.7(6)	2
Si1–Si1	231.0(2)	2	Mg1–Mg22	345.0(5)	2	Mg3–Ca2	295.6(7)	2
Si1–Si2	232.1(2)		Mg1–Ca2	362.8(1)	4	Mg3–Si2	303.5(7)	2
Si1–Ca2	319.0(1)	4	Mg1–Mg1	391.9(7)		Mg3–Mg1	306.4(11)	
Si1–Ca1	319.1(1)	2				Mg3–Mg22	338.7(4)	4
			Mg21–Mg22	69.7(5)				
Si2–Si1	232.1(2)		Mg21–Si2	279.2(1)	4			
Si2–Mg1	260.5(3)	2	Mg21–Mg1	294.7(3)	4			
Si2–Mg21	279.2(1)	2	Mg21–Ca2	351.0(1)	4			
Si2–Mg22	287.7(2)	4	Mg21–Si3	366.5(5)	2			
Si2–Mg3	303.5(7)	2	Mg21–Mg3	389.2(2)	8			
Si2–Ca2	319.5(1)	4						
Si2–Si2	342.3(3)							

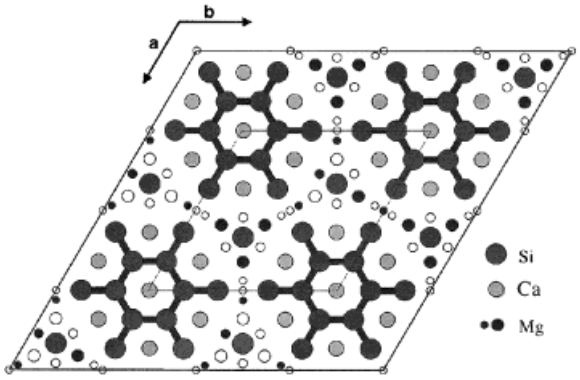

Figure 5. Projection of a possible ordered model of $Ca_7Mg_{7.5\pm\delta}Si_{14}$ along [001].

the standard deviation of the refined Mg content. We believe this is tolerable for such a model structure. This is the reason for the formulation $Ca_7Mg_{7.5\pm\delta}Si_{14}$, which is not so much indicative of a phase width as of the insecurity of the experimental composition. Despite numerous synthetic attempts we could not find any indication for a stoichiometric variation other than within the boundaries given here. The chemical analysis is not as reliable as the structural investigations because very small amounts of $CaSi_2$ impurities cannot be excluded. If the number of electrons is reduced, by replacement of magnesium by lithium, a completely different compound with the composition $Ca_7Li_{1.4}Mg_{2.6}Si_8$ results that does not contain silicon rings.[27]

Although the formal average charge of silicon in $Ca_7Mg_{7.5\pm\delta}Si_{14}$ is close to -2, it neither contains the linear chains found in MSi (M = Ca, Sr, Ba) nor the functionalized chain of $SrMgSi_2$ with (3b) Si^-, (2b) Si^{2-}, and (1b) Si^{3-}. (The expression (*n*b) indicates that there are *n* bonds assigned to the atomic center in question.) The formula may be split into cations and Zintl anions according to $(Ca_7Mg_{7.5\pm\delta})^{(29\pm2\delta)+}$-$[Si_{12}]^{(21\pm2\delta)-}(Si^{4-})_2$. The isolated Si^{4-} anions are predominantly coordinated to Mg atoms with some quite close contacts (258.7 pm). Such short distances have also been observed in other ternary silicides like Li_8MgSi_6 (253.7, 257.1 and 259.7 pm, ref. [34]). Some of the statistically occupied Mg sites are so close that they exclude each other and they cannot be occupied at the same time. Several reasonable local coordination models can be generated for the isolated Si3 atom. A completely ordered model may be derived for a fourfold unit cell in which *a* and *b* axes are doubled. Such a model was used for the quantum mechanical band-structure investigations (Figure 5).

On screening many different ternary alkaline earth metal silicides of magnesium the following trend can be found: the small, hard and polarizing Mg^{2+} stabilizes highly charged silicon atoms that are either terminally coordinated or isolated. On the other hand, the larger and softer Ca^{2+}, Sr^{2+}, and Ba^{2+} prefer highly interconnected, low-charged silicon atoms. In the case of $Ca_7Mg_{7.5\pm\delta}Si_{14}$ these trends are also observed. The isolated Si^{4-} and the singly bonded terminal Si in the Si_{12} group are coordinated by one Ca and four Mg sites, whereas the silicon atoms in the six ring of the Si_{12} group are exclusively surrounded by calcium. This central unit is a fragment of the AlB_2 structure in which the silicon atoms of the ring are found at the center of trigonal prisms of Ca atoms. This building block motif changes at the terminal Si atoms into a square antiprism (Mg_4Ca_4).

The displacements of the Si atoms of the Si_{12} unit have a quite peculiar pattern that cannot be explained by thermal movement. However, consideration of the disorder of Mg^{2+} cations provides a means of explanation. This may lead to concerted movements displayed in Scheme 1. Such deformations are reasonable. This is supported by the fact that no rigid

  0947-6539/98/0411-2254 $ 17.50+.50/0 *Chem. Eur. J.* **1998**, *4*, No. 11

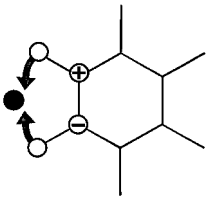

Scheme 1. Concerted thermal movement, as an explanation of the observed displacement parameters of the Si atoms in the Si_{12} unit.

group libration of the complete Si_{12} group can explain the observed displacement ellipsoids.

According to the observed composition and the result of the X-ray structure analysis there are 28.5 valence electrons available from Ca and Mg atoms to fill up the electronic states of the silicon entities. This leads to the formulation of a formally highly charged $Si_{12}^{(21\pm2\delta)-}$ anion and thus to a $(69\pm2\delta)$ electron system that is neither compatible with a benzenelike unit (66 e, Si_{12}^{18-}) nor with an exclusively singly bonded unit (72 e, Si_{12}^{24-}). According to the way in which the π-states for the planar system are filled, there are about 1.75 double bonds equally distributed over the whole six-membered ring. The bond distances are slightly shorter than single bonds, indicating a partial double-bond character. A riding correction on the basis of the displacement ellipsoids changes the slightly shorter intra-ring distance from 231.0 to 235.6 pm and the terminal contact from 232.2 to 236.4 pm. The relatively small difference between these distances might give rise to the assumption of completely delocalized π interactions, but the quantum mechanical calculations show that the terminal bonds have practically complete σ-bond character. It may be surprising that the Si_{12} unit exhibits a D_{6h} symmetry or at least is very close to it, if possible local deformations indicated by the displacement parameters are considered as well. There are some other examples of this kind indicating that isometric arrangements of Si six-membered rings with partially filled π* systems may be the preferred situations in anions of main group elements: $Ca_7Mg_{7.5\pm\delta}Si_{14}$, $n_e(\pi^*)=3\pm2\delta$; K_4P_6,[35] $n_e(\pi^*)=4$; $Ba_4Li_2Si_6$,[36] $n_e(\pi^*)=4$; $Ca_2Li_{1.7}Si_4$,[37] $n_e(\pi^*)=3.6$.

Theoretical investigations: In order to get a deeper insight into the electronic structure of the compound, theoretical investigations based on the semiempirical extended Hückel (EHMO)[38] and the first principles TB-LMTO-ASA methods[39] have been performed. Due to the partial occupancy of the Mg positions in the crystal structure, we had to derive an ordered model in a larger elementary cell ($a'=2a$, $b'=2b$, $c'=c$, see Figure 5). This model avoids unreasonable distances and generates suitable coordination spheres for all positions. The cumulated occupancies and thus the stoichiometry $Ca_7Mg_{7.25}Si_{14}$ are just within twice the standard deviation of the refined Mg content, which is tolerable. In the EHMO calculations the standard parameters for Ca, Mg, and Si are used and *k*-space integrations were performed on a set of 72 irreducible *k* points.[40]

The LMTO-ASA calculations were based on the LDA approximation with an exchange-correlation potential from Barth and Hedin.[41] The radii of the overlapping muffin-tin spheres in the ASA approximation were chosen as described by Jepsen and Andersen.[42] The basis consists of Si, Mg, Ca, and interstitial empty sphere s- and p-LMTOs with the d-partial and the p-partial waves of the interstitials folded into their tails. The energy expansion parameters $E_{\nu,RL}$ were chosen to be at the centers of gravity of the occupied part of the partial state densities. The *k*-space integrations were performed on a set of 167 irreducible *k* points. In order to get an initial idea of the bonding situation in $Ca_7Mg_{7.25}Si_{14}$ we calculated the distribution of the electron localization function (ELF) in selected cuts through the structure (Figure 6).

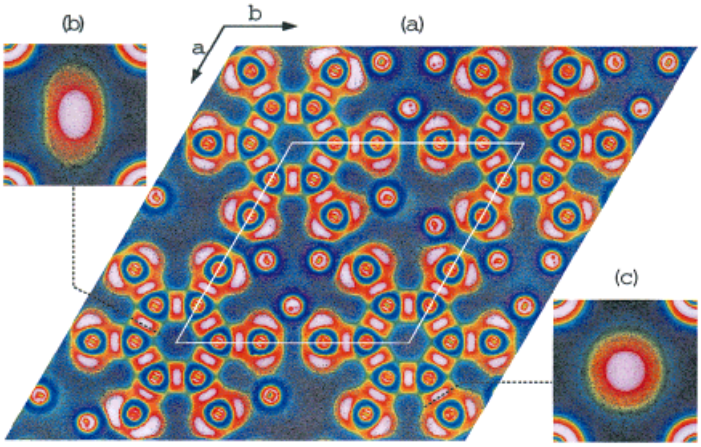

Figure 6. LMTO-ELF distribution in selected cuts through the structure of $Ca_7Mg_{7.5\pm\delta}Si_{14}$.[50]

The ELF distributions shown here are based on the LMTO wavefunction, but it has to be mentioned that the same qualitative pictures are yielded within the EHMO scheme. As has been shown recently, the ELF is a valuable tool with respect to an understanding of the bonding properties of individual molecules and of bulk materials in the solid state.[43] We find a high localization (ELF = 0.8–1.0, white) only in the region of the Si atoms. Inside the plane of the planar Si_{12} ring, the isolated Si_{12} moiety with bonds and lone-pairs is clearly outlined through structured regions of high localization (Figure 6a). Due to the unsymmetric magnesium distribution within the local model the D_{6h} symmetry of the Si_{12} is lost. This is reflected in the slightly different polarization of the lone pairs of the external Si atoms depending on the local Mg coordination. A comparison of the ELF distributions in cuts rectangular to the intra-ring Si–Si bond (Figure 6b) and the terminal Si–Si bond (Figure 6c) shows quite nicely the difference between the isotropic terminal Si–Si single bond and the elliptical intra-ring Si–Si bond with significant π participation. This picture is consistent with a formal charge transfer from the metal atoms to the Si substructure in the context of the Zintl–Klemm concept. Both EHMO and LMTO calculations do not show a bandgap (Figure 7) and predict metallic behavior for the compound. This corresponds very well with the results of the electrical conductivity measurement (Figure 1), in which the temperature dependence shows the characteristic behavior of a metal.

To shed further light on the metallic behavior we analyzed the EHMO band structure and the density of states (DOS) close to the Fermi energy (E_F) in a more detailed way (Figure 8). To do this we performed a fragment orbital analysis with respect to the orbital contributions of the isolated Si_{12} moiety. According to its symmetry the six highest π orbitals of Si_{12} may be labeled as $2a_{2u}$, $2e_{2g}$, $2e_{2u}$, and $2b_{2g}$

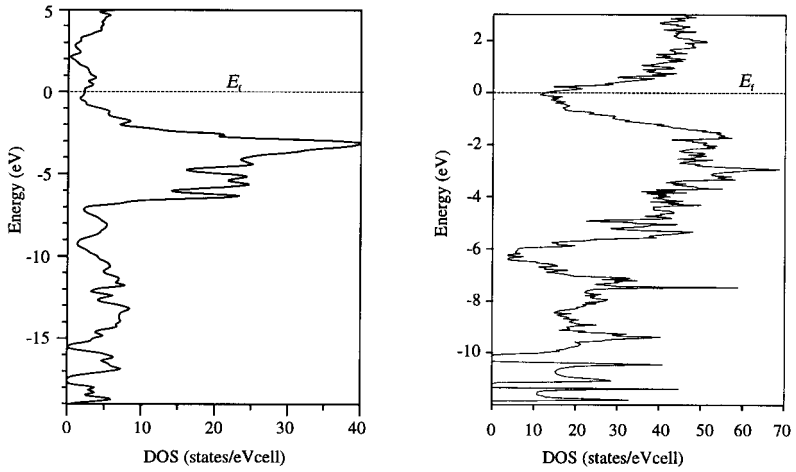

Figure 7. Comparison of the electronic density of states of EHMO (a) and LMTO (b) calculations on $Ca_7Mg_{7.25}Si_{14}$.

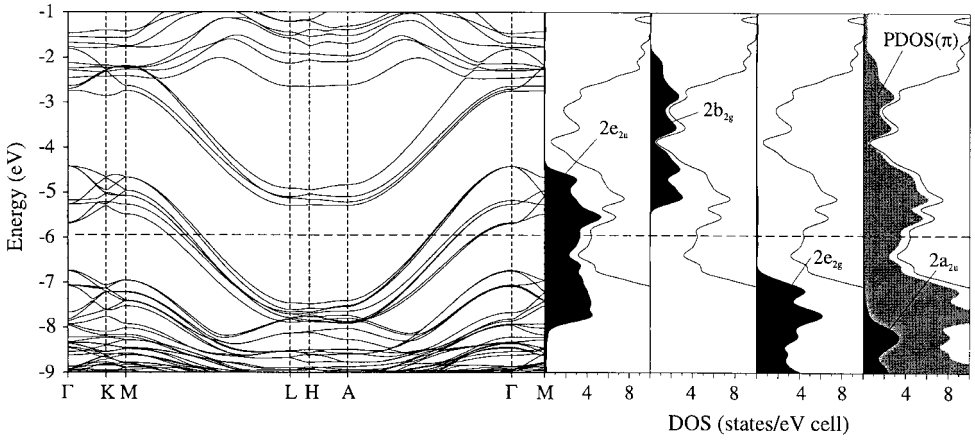

Figure 8. Section of the band structure and DOS based on EHMO calculations on $Ca_7Mg_{7.25}Si_{14}$ with corresponding projections on the π levels.

occupied states are exclusively centered at silicon. PED centered at calcium or magnesium is only found for energy windows above E_F. Thus the separation into $Si_{12}^{20.5-}$ (or $Si_{12}^{(21\pm2\delta)-}$, if one takes into account the refined Mg content) and isolated Si^{4-} proves to be a reasonable working scheme in the context of the Zintl–Klemm concept. One has to emphasize that this kind of view does not refer to a real charge distribution, but only considers the character of the states below the Fermi level. However, the formulation of $Si_{12}^{20.5-}$ only makes sense in the band structure picture because this special electron count is the result of the one-dimensional character of the stack of rings $^1_\infty[Si_{12}^{20.5-}]$.

Integer electron counts that have to be applied for quasi-isolated species can only occur here if a disproportionation develops, for example, Si_{12}^{20-} and Si_{12}^{21-}. This may actually be the case at lower temperatures, but has not been proved yet. The abnormalities of the resistivity and magnetic measurements at about 50 K could be interpreted in terms of such a phase transition leading to a Peierls type distortion and subsequent localization of conduction electrons.

Acknowledgments: This work was supported by the Swiss National Science Foundation (project No. 0-20-851-94) and the C4-project of the ETH Zurich.

Received: March 2, 1998 [F1035]

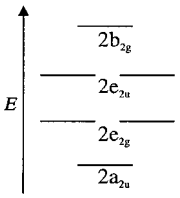

Scheme 2. MO scheme of the six highest π orbitals of the Si_{12} unit.

(Scheme 2). A quasi-aromatic Si_{12}^{18-} would have the π configuration $2a_{2u}^2 2e_{2g}^4$.

Obviously the bands close to the Fermi level are mainly built up of the π orbitals of the Si_{12} fragment, namely the $2e_{2g}$ and $2e_{2u}$ orbitals. In the c^* direction (e.g., $\Gamma \rightarrow$A or L $\rightarrow$M, ref. [44]) these π bands show a considerable dispersion based on a weak interaction of the ecliptically arranged Si_{12} moieties along the stacking direction. Due to this dispersion the energetic ranges of the different π levels overlap in such a manner that no special electron occupation is favored. A metallic behavior is expected in any case. As one can see from the DOS projections, the contributions of the $2a_{2u}$ and $2e_{2g}$ orbitals are clearly below the Fermi level and thus fully occupied, while the antibonding $2b_{2g}$ orbitals are unoccupied. The remaining antibonding $2e_{2u}$ levels are only partially filled and are responsible for the density of states at the Fermi level. Thus a strong anisotropy of the conductivity, for example, a one dimensional conductivity, is expected.

Inspections of partial electron density (PED[45, 46]) for energy windows below and above E_F clearly reveal that all

[1] O. Zmii, E. I. Gladyshevskii, in *2nd All-Union Conference on the Crystallochemistry of Intermetallic Compounds, Collected Abstracts* **1974**, 23.
[2] E. Zintl, *Angew. Chem.* **1939**, *52*, 1.
[3] E. Zintl, G. Brauer, *Z. Phys. Chem. B* **1933**, *20*, 245.
[4] W. Klemm, *Proc. Chem. Soc. London* **1958**, 329.
[5] E. Mooser, W. B. Pearson, *Progress in Semiconductors*, *Vol. 5*, Wiley, New York, **1960**.
[6] E. Busmann, *Z. Anorg. Allg. Chem.* **1961**, *313*, 90.
[7] W. Klemm, *Festkörperprobleme Bd. III*, Vieweg, Braunschweig, **1963**.
[8] H. Schäfer, B. Eisenmann, W. Müller, *Angew. Chem.* **1973**, *85*, 742; *Angew. Chem. Int. Ed. Engl.* **1973**, *12*, 694.
[9] J. Evers, G. Oehlinger, A. Weiss, *J. Solid State Chem.* **1977**, *20*, 173.
[10] J. Evers, *J. Solid State Chem.* **1979**, *28*, 369.
[11] J. Evers, *J. Phys. Chem. Solids* **1979**, 40, 951.
[12] J. Evers, G. Oehlinger, A. Weiss, *Z. Naturforsch. B* **1982**, *37*, 1487.
[13] R. Nesper, A. Currao, S. Wengert, *Organosilicon Chemistry, From Molecules to Materials, Vol. II*, VCH, Weinheim **1995**, p. 469ff.
[14] A. Currao, J. Curda, R. Nesper, *Z. Anorg. Allg. Chem.* **1996**, *622*, 85.
[15] E. N. Nikitin, E. N. Tkalenko, V. K. Zaitsev, A. I. Zaslavskii, A. K. Kuznetsov, *Inorganic Materials* **1968**, *4*, 1656.
[16] H. Witte, *Naturwissensch.* **1937**, *25*, 795.
[17] K. Turban, H. Schäfer, *Z. Naturforsch. B* **1973**, *28*, 220.
[18] B. Eisenmann, H. Schäfer, *Z. Naturforsch. B* **1974**, *29*, 13.
[19] E. Hellner, *Z. Anorg. Allg. Chem.* **1950**, *261*, 226.
[20] E. Hellner, *Angew. Chem.* **1950**, *62*, 125.
[21] G. Rocktäschel, A. Weiss, *Z. Anorg. Allg. Chem.* **1962**, *316*, 231.

  0947-6539/98/0411-2256 $ 17.50+.50/0 *Chem. Eur. J.* **1998**, *4*, No. 11

[22] W. Rieger, E. Parthé, *Acta Crystallogr.* **1967**, *22*, 919.
[23] J. Böhm, O. Hassel, *Z. Anorg. Allg. Chem.* **1927**, *160*, 152.
[24] K. H. Janzon, H. Schäfer, A. Weiss, *Z. Naturforsch. B* **1968**, *23*, 1544.
[25] A. Currao, S. Wengert, R. Nesper, J. Curda, H. Hillebrecht, *Z. Anorg. Allg. Chem.* **1996**, *622*, 501.
[26] J. R. Wynnyckyj, L. M. Pidgeon, *High Temp. Sci.* **1972**, *4*, 192.
[27] A. Currao, Dissertation No. 11747, ETH Zürich **1996**.
[28] H. Axel, B. Eisenmann, H.Schäfer, A.Weiss, *Z. Naturforsch. B* **1969**, *24*, 815.
[29] B. Eisenmann, H. Schäfer, A. Weiss, *Z. Anorg. Allg. Chem.* **1972**, *391*, 241.
[30] A. Weiss, H. Witte, *Magnetochemie, Grundlagen und Anwendungen*, VCH, Weinheim **1973**, p. 94ff.
[31] Further details of the crystal structure investigation can be obtained from Fachinformationszentrum Karlsruhe, D-76344 Eggenstein-Leopoldshafen (Germany), (fax: (+49) 7247-808-666; e-mail: crysdata@fiz.karlsruhe.de) on quoting the depository number CSD-408375.
[32] G. M. Sheldrick, SHELXS: Program for the Solution of Crystal Structures, Göttingen **1985**.
[33] G. M. Sheldrick, SHELXL96: Program for the Refinement of Crystal Structures, Göttingen **1996**.
[34] R. Nesper, J. Curda, H. G. von Schnering, *J. Solid State Chem.* **1986**, *170*, 199.
[35] H.-P. Abicht, W. Hönle, H. G. von Schnering, *Z. Anorg. Allg. Chem.* **1984**, *519*, 7.
[36] H. G. von Schnering, U. Bolle, J. Curda, K. Peters, W. Carillo-Cabrera, M. Somer, M. Schultheiss, U. Wedig, *Angew. Chem.* **1996**, *108*, 1062; *Angew. Chem. Int. Ed. Engl.* **1996**, *35*, 984.
[37] W. Müller, H. Schäfer, A. Weiss, *Z. Naturforsch. B* **1970**, *25*, 1371.
[38] U. Häussermann, R. Nesper, S. Wengert, T. F. Fässler, Program MEHMACC: modified Extended-Hückel version based on the QCPE programm EHMACC,[47] ETH Zürich, **1993**.
[39] G. Krier, O. Jepsen, A. Burkhardt, O. K. Andersen, TB-LMTO-ASA Program, MPI für Festkörperforschung, Stuttgart, **1994**.
[40] Ca: $H_{ii}(4s) = -7.0$, $\zeta(4s) = 1.20$, $H_{ii}(4p) = -4.0$, $\zeta(4p) = 1.20$; Mg: $H_{ii}(3s) = -9.0$, $\zeta(3s) = 1.38$, $H_{ii}(3p) = -4.5$, $\zeta(3p) = 1.38$; Si: $H_{ii}(3s) = -17.3$, $\zeta(3s) = 1.10$, $H_{ii}(3p) = -9.2$, $\zeta(3p) = 1.10$.
[41] U. Bart, L. Hedin, *J. Phys. C* **1972**, *5*, 1629.
[42] O. Jepsen, O. K. Andersen, *Z. Phys. B* **1995**, *97*, 35.
[43] A. Savin, R. Nesper, S. Wengert, T. Fässler, *Angew. Chem.* **1997**, *109*, 1892; *Angew. Chem. Int. Ed. Engl.* **1997**, *36*, 1808.
[44] C. J. Bradley, A. P. Cracknell, *The Mathematical Theory of Symmetry in Solids*, Clarendon, Oxford **1972**.
[45] T. F. Fässler, U. Häussermann, R. Nesper, *Chem. Eur. J.* **1995**, *1*, 625.
[46] S. Wengert, Dissertation ETH No. 12070, ETH Zürich, **1997**.
[47] M.-H. Wangbo, M. Evain, T. Hughbanks, M. Kertesz, S. Wijeyesekera, C. Wilker, C. Zheng, R. Hoffmann, Program EHMACC: Extended Hückel Molecular and Crystal Calculations.
[48] E. Dowty, ATOMS, Computer Program for Displaying Atomic Structures, Shape Software, version 3.1 for windows edition **1995**.
[49] A. Larson, F. L. Lee, Y. Le Page, M. Webster, J.-P. Charland, E.Gabe, NRCVAX Crystal Structure System Interactive Version of ORTEPII, NRC, Ottawa (Canada) **1986**.
[50] J. Flad, F.-X. Fraschio, B. Miehlich, Programm GRAPA, Institut für Theoretische Chemie der Universität Stuttgart.
[51] W. Clegg, *Acta Crystallogr. A* **1981**, *37*, 22.

  0947-6539/98/0411-2257 $ 17.50+.25/0